Journal of Computational Applied Mechanics 2023, 54 (1): 111-126

DOI: 10.22059/JCAMECH.2023.353492.791

RESEARCH PAPER

Thermal Radiation and Magnetic Fields Effects on Nanofluids Flowing Through Stretch Sheet

Chandu.M.Koli [a,*], S.N.Salunkhe [b]

[a] *Department of Applied Science, SVKM Institute of Technology, Dhule, India.*
[b] *Rani Laxmibai Mahavidyalaya Parola, Jalgaon, India*

Abstract

The purpose of the present study is to observe when the presence of suction/injection, thermophoresis, and Brownian motion effects, this research paper emphasises the combined impact of heat radiation and magnetic field on convective nanofluid flow towards a permeable stretched sheet. The Rosseland approximation is applied to describe the radiative heat flux in the heat convective analysis. The radiative heat transfer is practically applicable in hypersonic flights, nuclear power plants, space vehicles, gas turbines, nuclear reactors, the model of pertinent equipment etc. The boundary wall takes into account stretching and suction/injection circumstances. The dimensionless version of basic governing equations is simplified using a non-dimensionalization method. Runge-Kutta technique is used to solve the final version of the fundamental equations numerically. The changes of velocity, temperature, and concentration fields versus different physical constraints are examined via graphical data demonstrations. The changing trends of heat and mass transfer rates, as well as the skin- friction coefficient, are also studied using numerical data. The proposed model is additionally validated by comparing it to a limited instance of a previously researched issue..

Keywords: Thermal radiation; Magnetic field; Nanofluid; Stretching sheet; Runge-Kutta technique

1. Introduction

Recent research has concentrated on the boundary layer flow of an electrically conducting nanofluid toward a stretched sheet, which has been seen in many experiments. In the context of nanofluids, a fluid composed of a homogeneous suspension of nano/micro-sized solid particles (metal/nonmetal/nanofibers) in a conventional base fluid, with a typical size of less than 100 nm, is defined as follows: (liquid). This includes a variety of techniques such as the adding of minute solid particles to the liquid. Stretching boundary-induced flow has a broad variety of applications in extrusion processes used in the plastic and metal industries, among other things. Lin, Y., et al., [1] developed an unsteady flow and heat transmission across a stretched surface using the heat and unsteady flow of MHD pseudo-plastic nanofluid transmission model into a finite skinny film by internal heat generation. Zhang, C., et al. [2], investigated heat flux and chemical reaction and radiation heat transfer Nanofluids MHD flow of in porous media by variable surface. Radiation impacts on heat transfer and Marangoni convection flow in pseudo-plastic non-Newtonian Variable thermal conductivity discussed by Lin, Y., L. Zheng, and X. Zhang [3].Mabood, F., et al. [4], examined Nanofluids non-Darcian convective flow through a stretching sheet within a micropolar fluid radiation with non-uniform heat source/sink and Soret effects.. Seth, G.S., et al. [5],described the heat-absorbing and

* Corresponding author. *E-mail address:* mkolichandu@gmail.com

radiating fluid flowing hydromagnetically across an exponentially stretched sheet with partial slip, viscous, and Joule dissipation. Anjali Devi, S.P. and M. Prakash [6], looked into theTemperature dependent viscosity and thermal conductivity effects on hydromagnetic flow over a slendering stretching sheet. Hayat, T., et al., [7] examined Williamson nanofluid flow in two dimensions was studied in conjunction melting of a nonlinear variable thickness surface heat transfer. Effects of MHD heat transfer flowin Homogeneous-heterogeneous reactions and melting by variable thickness through stretching surface looked by Hayat, T., et al. [8]. Farroq and colleagues [9] investigate the in a MHD flow on nanofluid viscoelastic with non-linear radiation effects. MHD stagnation flow through viscous dissipation and Joule heating of Modified homogeneous-heterogeneous reactions presented by Khan, M.I., et al [10]. Hayat, T., et al. [11], look into Effectiveness of magnetic nanoparticles in Eyring-Powell fluid radiative flow. Hayat, T., et al. [12], observed Effect of magnetonano fluid flow viscous dissipation with variable properties. Hayat, T., et al. [13], discussed Thermal radiation effect of Marangoni convection in the flow of nanofluid carbon–water. Radioactive nonlinear Numerical simulation flow by convective cylinder looked by Hayat, T., et al [14].Tamoor, M., et al. [15], presented Casson fluid magnetohydrodynamic flow over a stretching cylinder. Babu, N., G. Murali, and S. Bhati, [16] discussed Casson fluid performance with Natural convective dissipative couette flow hall current, heat transfer and MHD impact on past an infinite vertically inclined plate filled within porous medium. Murali, G., A. Paul, and N. Babu, [17] used the effects of Unsteady heat absorption hydromagnetic free convective flow of heat and mass transfer embedded over infinite vertical plate in porous medium. Thermal radiation and chemical reaction in an infinite vertical plate of unsteady hydromagnetic mixed convection flow examined by Gadipally, D., M. Gundagani, and N.N. Babu [18]. Mohammadi et al. [19-60] analysed the mechanical nanostructured.

It is concluded based on the literature cited above that the principle of the analysis is to determine the extent to which heat radiation going on a non-linearly stretched sheet using a magnetohydrodynamic model that incorporates Brownian motion and effects of thermophoresis, building on the findings of the aforementioned reference work. The numerical solution of the modified basic governing equations is accomplished used by Runge- Kutta technique, which employs a set of dimensionless variables. Several significant physical embedded parameters for the domains of velocity, temperature, and concentration by using graphical representation in the respective domains. Important Physical quantities, like the local skin-friction coefficient, the local Nusselt and Sherwood numbers, and etc, were determined numerically by referring to online tables of values. Aeronautical, Civil, Mechanical and Marine constructions and designs are all covered by this non-linear stretching sheet.

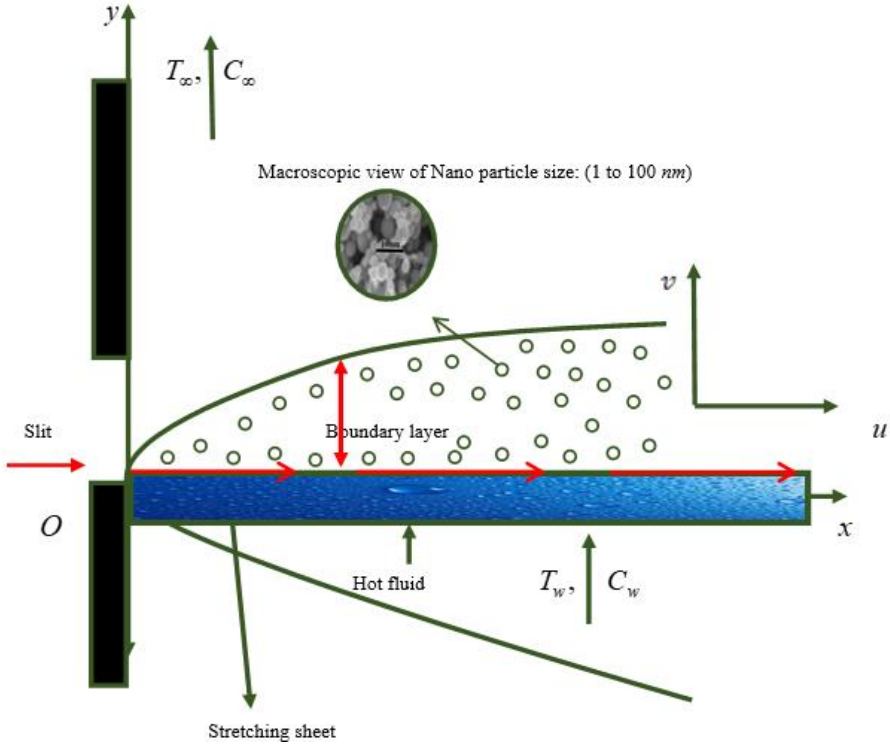

Fig. 1.: The fluid's is represented by geometry.

2. Flow Governing Equations:

In this research work, an incompressible and viscous nanofluid on a two-dimensional, steady, electrical conducting, nonlinearly permeable sheet with thermal radiation is investigated. For this flow, the flow geometry is shown in the Fig1. for this research work, the following assumptions are considered for this investigation:

i. It is assumed that the problem's geometry is represented in the coordinate system has horizontal X-axis and a perpendicular Y-axis

ii. We consider study 2-dimensional boundary layer flow through a stretching sheet.

iii. Additionally, we considered the flow of nanofluids when into the presence of a magnetic field normal to the nanofluids and the flow was placed at $y \geq 0$; here y is the coordinate measured normal to the stretching surface.

iv. The temperature T and volume concentration C of nanoparticles at the boundaries are assumed to be T_w and C_w , respectively, at the wall T_∞ and C_∞ , respectively are far-away from the wall.

v. Also, it is thought that there will be less of a temperature gradient in the flow of viscous fluid so that T^4 temperature can be stated when a linear function. Expansion of T^4 by Taylor's method, move towards on a temperature of free stream T_∞ .

vi. It is supposed that the sheet shrinks exponentially through velocity $u_w(x) = U_w \exp\left(\frac{x}{L}\right)$.

vii. Moreover, The magnetic field B (x) is supposed

$$B = B_0 e^{\left(\frac{x}{L}\right)} \tag{1}$$

Based on the above assumptions, the incompressible and electrically conducting two-dimensional magneto hydrodynamic nanofluid the equation for the boundary layer flow is as follows:

Continuity Equation:

$$\left(\frac{\partial u}{\partial x}\right) + \left(\frac{\partial v}{\partial y}\right) = 0 \tag{2}$$

Equation of Momentum:

$$\left(\frac{\partial u}{\partial x}\right)u + \left(\frac{\partial u}{\partial y}\right)v = \left(\frac{\partial^2 u}{\partial y^2}\right)v - \left(\frac{\sigma B_0^2}{\rho}\right)u \tag{3}$$

Equation of thermal energy:

$$u\left(\frac{\partial T}{\partial x}\right) + v\left(\frac{\partial T}{\partial y}\right) = \alpha\left(\frac{\partial^2 T}{\partial y^2}\right) + \tau_B\left\{D_B\left(\frac{\partial C}{\partial y}\right)\left(\frac{\partial T}{\partial y}\right) + \left(\frac{D_T}{T_\infty}\right)\left(\frac{\partial T}{\partial y}\right)^2\right\} + \left(\frac{16\sigma^* T_\infty^3}{3k^* \rho C_p}\right)\left(\frac{\partial^2 T}{\partial y^2}\right) \tag{4}$$

Equation of species nanoparticle volume concentration:

$$u\left(\frac{\partial C}{\partial x}\right) + v\left(\frac{\partial C}{\partial y}\right) = D_B\left(\frac{\partial^2 C}{\partial y^2}\right) + \left(\frac{D_T}{T_\infty}\right)\left(\frac{\partial^2 T}{\partial y^2}\right) \tag{5}$$

The boundary conditions for this flow are

$$\left.\begin{array}{l} u_w(x) = U_w \exp\left(\frac{x}{L}\right),\ v_w(x) = V_o \exp\left(\frac{x}{2L}\right),\ T = T_w,\ C = C_w \ \ at \ \ y = 0 \\ u \to 0,\ v \to 0,\ T \to T_\infty,\ C \to C_\infty \ \ as \ \ y \to \infty \end{array}\right\} \tag{6}$$

Transformations of similarity are presented as follows

$$\left.\begin{aligned} &u = U_o \exp\left(\frac{x}{L}\right) f'(\eta),\ v = -\sqrt{\frac{\nu U_o}{2L}} \exp\left(\frac{x}{2L}\right)\left\{ f(\eta) + \eta f'(\eta)\right\}, \\ &\eta = y\sqrt{\frac{U_o}{2\nu L}} \exp\left(\frac{x}{2L}\right),\ \theta = \frac{T - T_\infty}{T_w - T_\infty},\ \phi = \frac{C - C_\infty}{C_w - C_\infty} \end{aligned}\right\} \tag{7}$$

Equation of continuity is satisfied identically when Eq. (7) is used, and Eqs. (3) to (5), as well as (7), take the form.

$$f''' + ff'' - Mf' - 2\left(f'^2\right) = 0 \tag{8}$$

$$\left(1 + \frac{4R}{3}\right)\theta'' + \Pr f\theta' - \Pr f'\theta + \Pr Nb\theta'\phi' + \Pr Nt\left(\theta'\right)^2 = 0 \tag{9}$$

$$Nb\phi'' + LeNb \Pr f\phi' - LeNb \Pr f'\phi + Nt\theta'' = 0$$

(10)

The corresponding boundary conditions (6) be transformed into

$$\left. f(0) = S,\ f'(0) = \lambda,\ \theta(0) = 1,\ \phi(0) = 1\ \&\ f'(\infty) \to 0,\ \theta(\infty) \to 0,\ \phi(\infty) \to 0 \right\}$$

(11)

Here physical parameters involved are specified

$$\left. M = \frac{2\sigma B_o^2 L}{\rho U_o},\ \lambda = \frac{U_w}{U_o},\ \Pr = \frac{\nu}{\alpha},\ R = \frac{4\sigma^* T_\infty^3}{3\kappa k^*}\ Nb = \frac{(\rho C)_p D_B (C_w - C_\infty)}{\nu (\rho C)_f},\ Nt = \frac{(\rho C)_p D_T (T_w - T_\infty)}{\nu(\rho C)_f} \right\}$$

(12)

The local Nusselt number, the local Sherwood number, and the physical parameters of the skin-friction coefficient are the relevant physical quantities.

$$Cf = \frac{\tau_w}{\rho U_w} \Rightarrow \mathrm{Re}_x^{-\frac{1}{2}}\, Cf = f''(0) \tag{13}$$

$$Nu_x = \frac{xq_w}{\kappa(T_w - T_\infty)} \text{ Where } q_w = -\left(\kappa + \frac{16\sigma^* T_\infty^3}{3k^*}\right)\left(\frac{\partial T}{\partial y}\right)_{y=0} \Rightarrow \mathrm{Re}_x^{-\frac{1}{2}}\, Nu_x = -\left(1 + \frac{4R}{3}\right)\theta'(0) \tag{14}$$

$$Sh_x = \frac{xq_m}{D_B(T_w - T_\infty)} \text{ Where } q_m = -D_B\left(\frac{\partial C}{\partial y}\right)_{y=0} \Rightarrow \mathrm{Re}_x^{-\frac{1}{2}}\, Sh_x = -\phi'(0) \tag{15}$$

Where $\mathrm{Re}_x = \dfrac{U_o x\left\{\exp\left(\dfrac{x}{L}\right)\right\}}{\nu}$ be the local Reynolds number.

3. Runge-Kutta technique Solutions:

An exact solution does not have seemed to be possible in the case of a full set of Eqs. (8)-(10).Preferred to use numerical methods to resolve the system of ordinary differential equations (8)-(10) and its initial and boundary conditions (11). [0, ∞) has been replaced with the bounded domain $\left[0,\ \eta_\infty\right]$ and here η_∞ be an appropriate a finite real number that must satisfies the domain. Preferred to use numerical methods to obtain a system of ordinary differential equations (8)-(10) and their associated initial and boundary conditions (11). (8)- (10) nonlinear initial boundary value problems for third and second order ODEs. Thus, the supposition in (8)-(10) was reduced to a system of 7 initial problems with 7 unknowns of the first order.

$$\left. f = y_1,\ f' = y_2,\ f'' = y_3,\ \theta = y_4,\ \theta' = y_5,\ \phi = y_6,\ \phi' = y_7 \right\} \tag{16}$$

Thus we used efficient numerical method Runge-Kutta shooting of the fourth order. Symbolic software MAPLE is used to solve the numerical problem. Because we have simply four initial conditions $f(0)$, $f'(0)$, $\theta(0)$ and $\phi(0)$, and three $f''(0)$, $\theta'(0)$ and $\phi'(0)$ other unknowns to work with, a numerical shooting method is used in which these three preliminary conditions are used to guess what three other initial conditions are needed to solve the system. When running a mathematical simulation, the step size should be $\nabla\eta = 10^{-3}$.The threshold for convergence is 10^{-8}.

4. Program Code Validation

In order to validation of programme code for verification, the current Nusselt number results are compared with published Nusselt number results of Magyari and Keller [61], Bidin and Nazar [62] and El-Aziz [63] in Table-1 in absence of Nanofluid as S = 0, λ = 1 and R = 0. As result of this table, data generated by the current code has been found and the data generated by the previous code are comparable in quality Magyari and Keller [61], Bidin and Nazar [62] and El-Aziz [63] show excellent the use of the current numerical code and agreement is justified.

Table-1.: a comparison of the experimentally obtained Nusselt number with the previously published one to see if there has been any variation in it when S = 0, λ = 1 and R= 0

Pr	Keller and Magyari [61]	Nazar and Bidin [62]	El-Aziz [63]	Present numerical results
1.0	0.9548	0.9547	0.9548	0.950122586145
2.0	--------	1.4714	--------	1.471020365516
3.0	1.8691	1.8691	1.8691	1.864203220154
5.0	2.5001	--------	2.5001	2.500001315466
10.0	3.6604	--------	3.6604	3.660136267784

5. Results and Discussion:

This research work considers the radiative steady, viscous, incompressible, electrically conducting Non-linearly stretching sheet under the influence of injection/ suction, Brownian motion, and Thermophoresis MHD flow of nanofluid. The numerical solution called Runge-Kutta method is used to solve the governing equations of the flow field. The flow is presided over by the non-dimensional parameters namely, Magnetic field parameter*M*,Suction/injection parameter *S*, Stretching parameter λ, Prandtl number Pr, Brownian motion parameter *Nb*, Thermophoresis parameter *Nt*, Thermal radiation parameter *R* and Lewis number *Le*. Figs. 2- 11 represented the profiles of velocity, temperature and nanoparticle concentration profiles correspondingly. Also,the numerical values of physical quantities such as, the skin friction, Nusselt numberand Sherwood number are also computed and displayed in Tables-2-4 respectively.

Fig. 2 Magnetic field parameter (M) effect is observed on velocity profiles. The velocities decrease as M increases in fig.2. Because the magnetic field presence in the system produces Lorenz force, supposed the force to disturb the heat dissipation of the fluid by retarding the rate of the heat transfer in the fluid. This causes the thermal boundary layer to become thicker as M increases.

Fig.3 demonstrates the suction/injection parameter's (S) effect on the dimensionless stream wise velocities (V). The graphs in Fig. 3 demonstrate that the thickness of the boundary layer is strongly influenced by the parameter S. The flow appears to slow significantly as S is raised. With suction/injection, this causes the boundary layer to be pushed closer to the wall, which decreases velocity. The momentum boundary layer's thickness is reduced as a result of the suction/injection.

Stretching rates between both directions y –, x – are measured by their ratio λ. As can be seen in Figure 4, increasing the stretching rate ratio parameter reduces in x-direction velocity while increasing in y-direction velocity

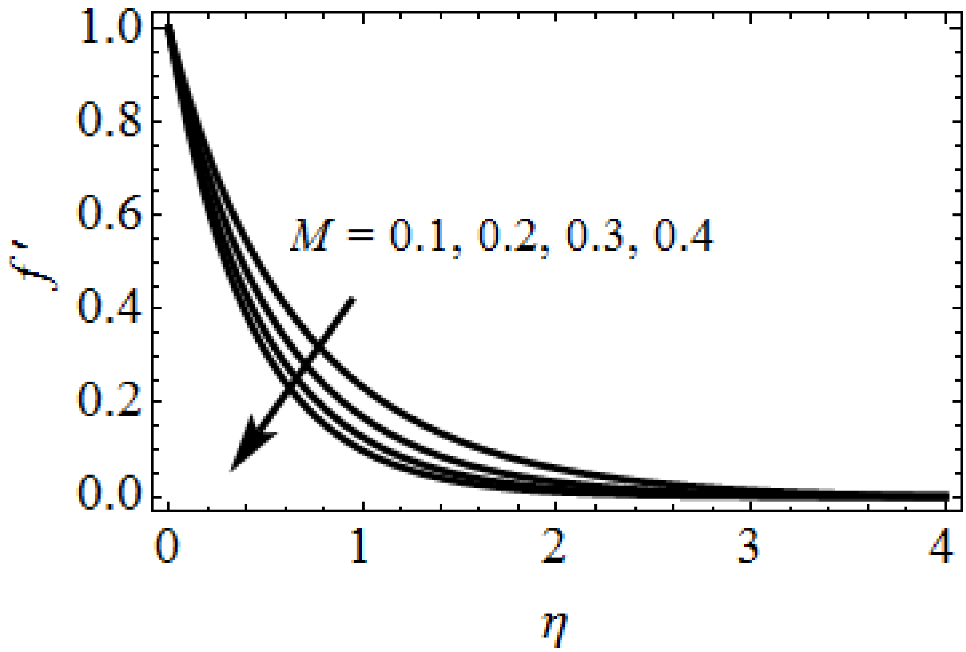

Fig. 2 The M effect is observed on velocity profiles

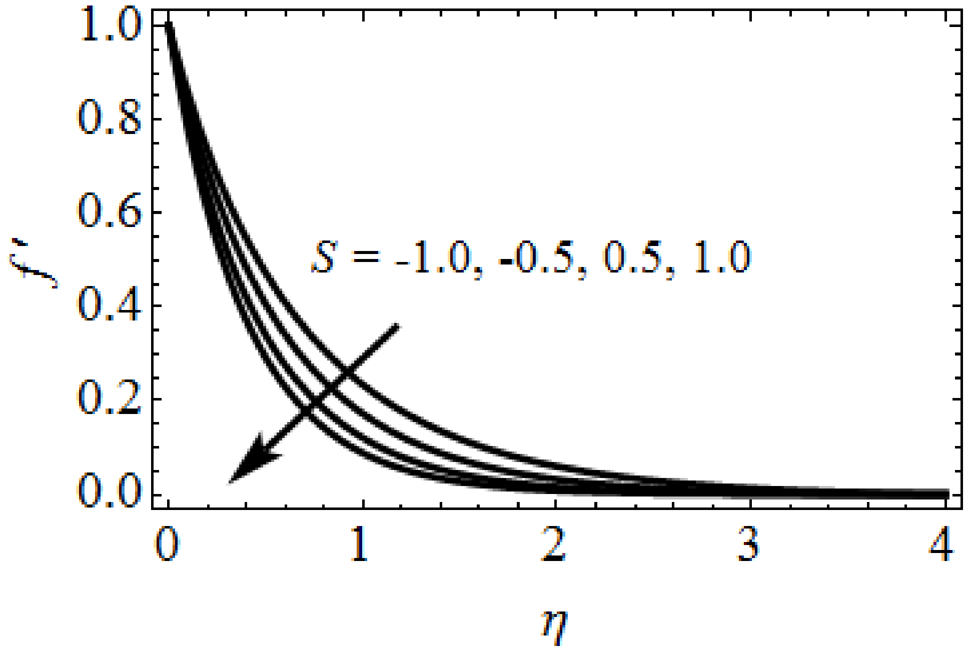

. **Fig. 3.** The S impact is observed on velocity profiles

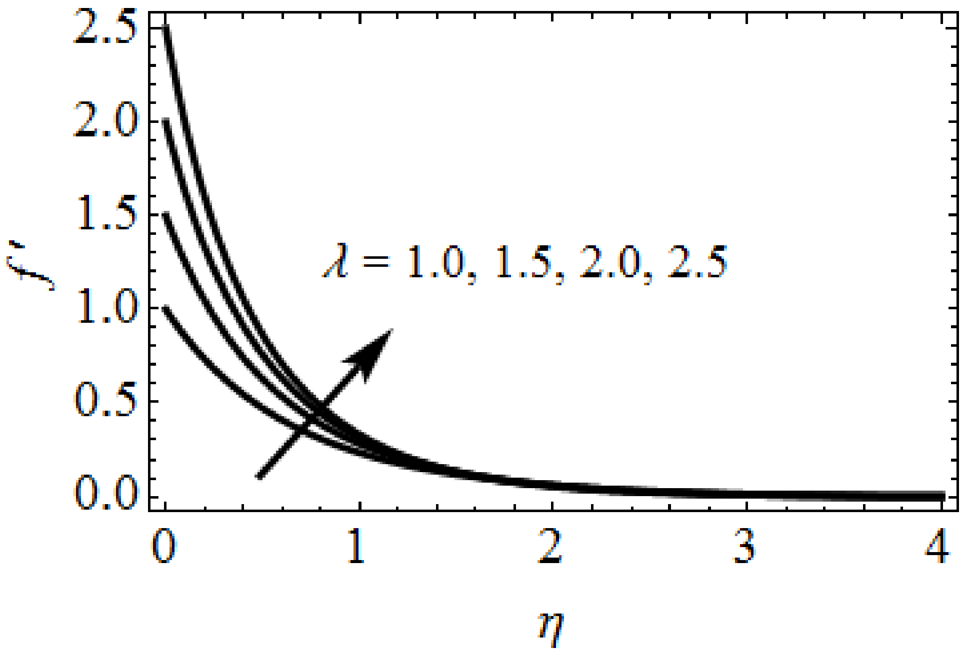

Fig. 4.λ effect on velocity profiles

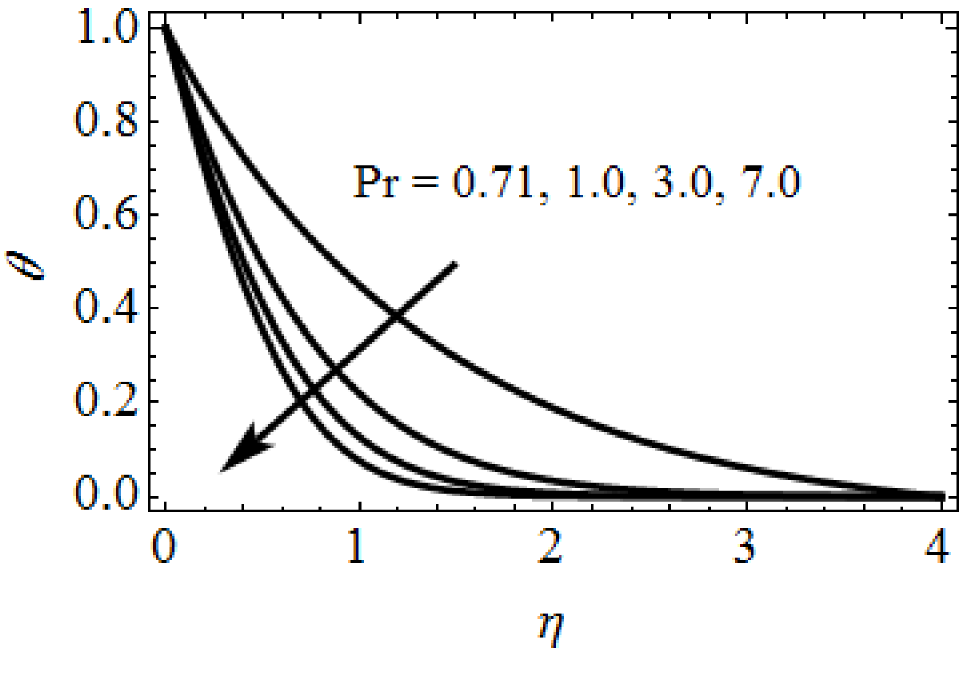

Fig. 5. Pr impact on temperature profiles

Prandtl number (Pr) an effect on fluid temperature in Fig.5 is shown. As Pr value raises, the temperature gradient in the fluid decreases. The thermal diffusivity increases and dominates the thermal diffusivity as Pr rises. The fluid velocity is high enough to help the heat transfer of the fluid. This makes the heat dissipation rate faster and makes the boundary layer to become thinner.

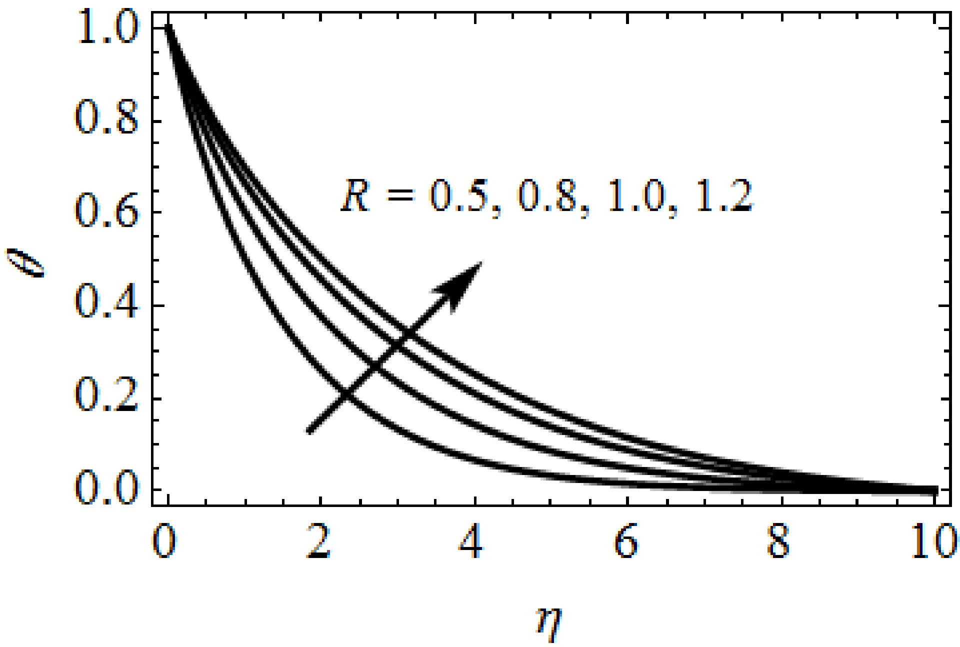

Fig. 6.*R* impact on temperature profiles

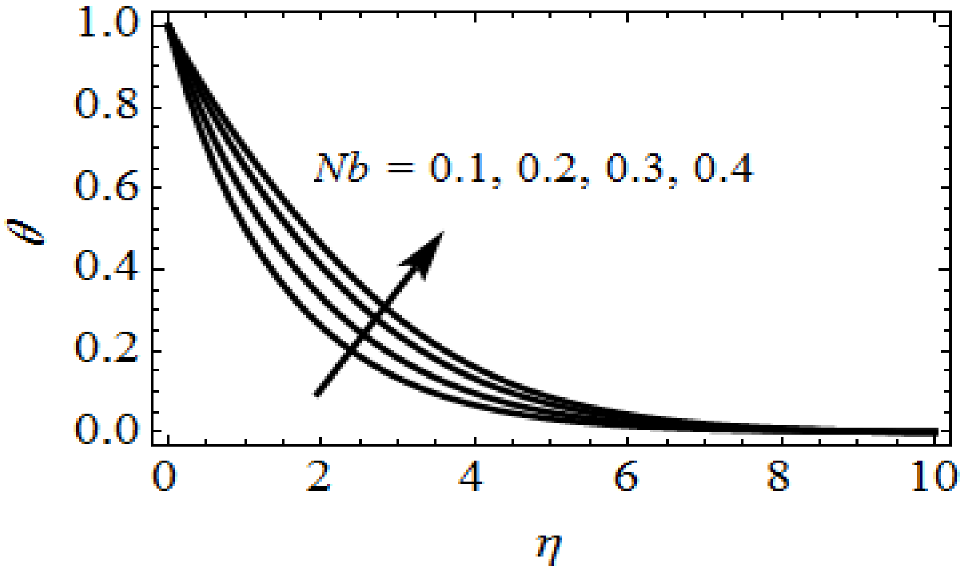

Fig. 7.*Nb* impact on temperature profiles

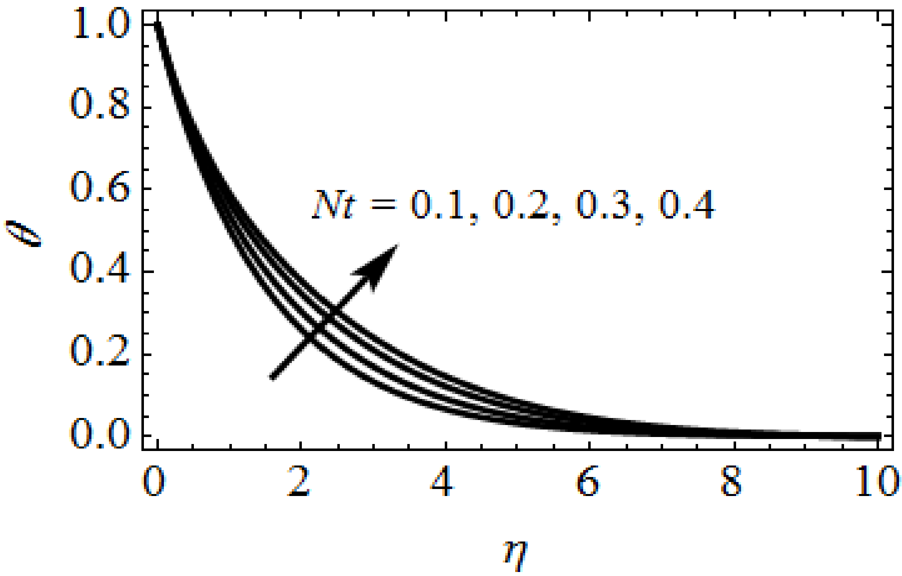

Fig. 8.*Nt* impact on temperature profiles

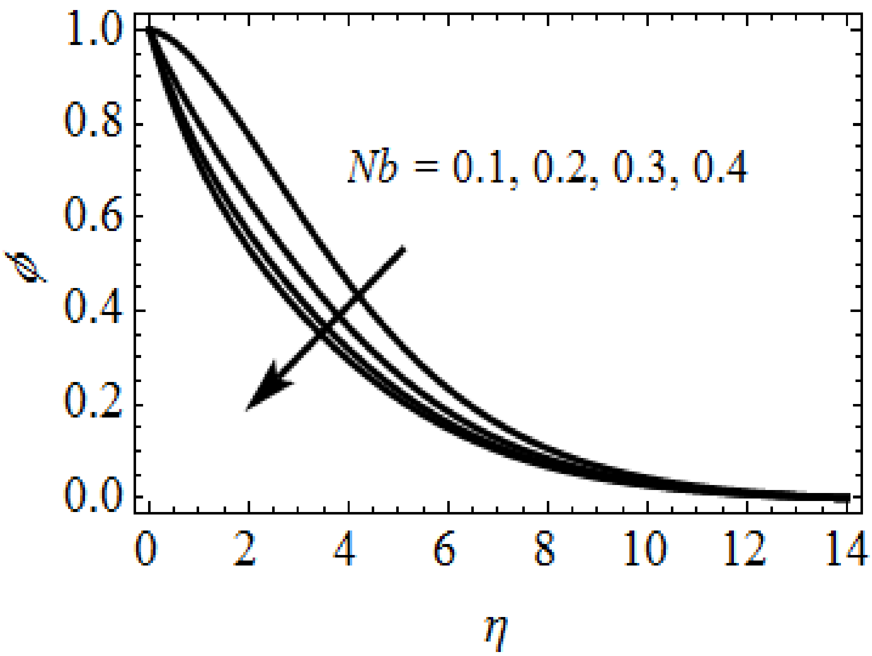

Fig. 9.*Nb* impact on nanoparticle volume Concentration profiles

The impact of thermal radiation parameter (R) on temperature field is illustrated in Fig. 6. It is observed from this Fig. 8 that, temperature of the fluid increases for the raising values of R. The growing values in the radiation parameter improve the conduction effects which as a result enhances the temperature field.

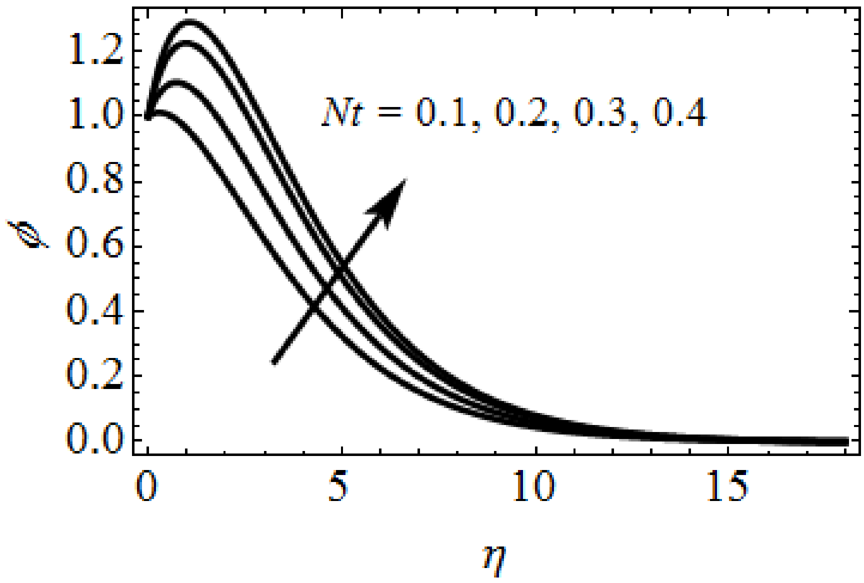

Fig. 10.*Nt* impact on nanoparticle Volume concentration profiles

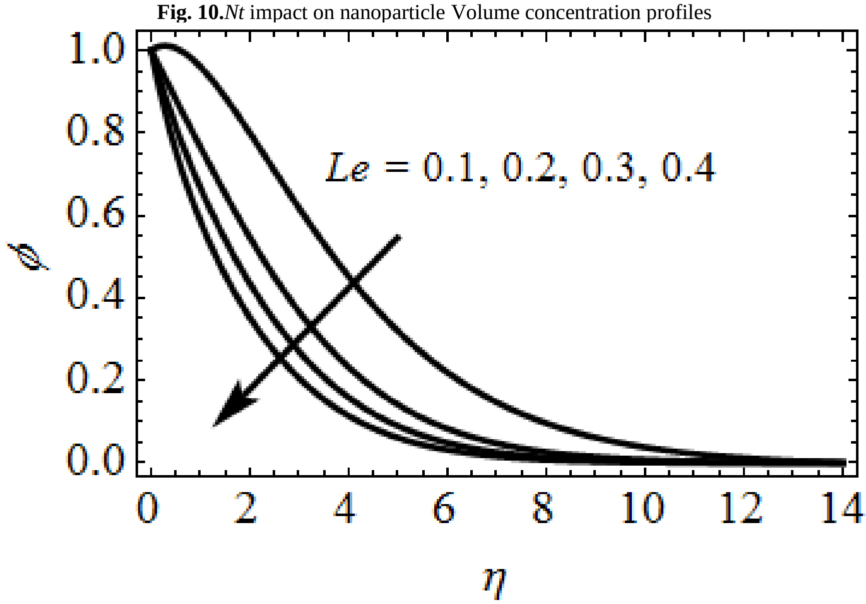

Fig. 11.*Le* impact on nanoparticle volume concentration profiles

Figs. 7 to 10 illustrate the effects of the Brownian motion parameter (*Nb*) and the Thermophoresis parameter (*Nt*) on the dimensionless temperature and nanoparticle volume concentration profiles respectively. It is observed that with increasing values of the Brownian motion parameter (*Nb*), the temperature profile increases and the nanoparticle volume concentration profile decreases. Further, we also notice that by increasing the value of the Thermophoresis parameter (*Nt*), the dimensionless temperature and nanoparticle volume fraction increase. This is due to the fact that the Thermophoretic force is produced by the temperature gradient and it creates a very high velocity flow away from the stretching sheet. In this way, the fluid is more heated and away from the stretching surface and consequentially, as the Thermophoresis parameter (*Nt*) increases, the thermal boundary layer thickness increases and the temperature gradient at surface decreases as both *Nt* and *Nb* values increase.

Table-2.: Different variations in the coefficient of skin friction are represented numerically. *M*, *S*, *λ*,Pr, *Nb*, *Nt*, *R* and *Le*

M	*S*	*λ*	Pr	*Nb*	*Nt*	*R*	*Le*	*Cf*
0.1	- 1.0	1.0	0.71	0.1	0.1	0.5	0.1	1.1823301544
0.2								1.1428851402
0.3								1.1269550396
0.4								1.1106298855
	-0.5							1.1563324011
	0.5							1.1390042516
	1.0							1.1236055042
		1.5						1.2355808967
		2.0						1.2536695482
		2.5						1.2690024785
			1.0					1.1395524846
			3.0					1.1082334755
			7.0					1.0830364757
				0.2				1.2085224687
				0.3				1.2263345051
				0.4				1.2563350245
					0.2			1.2036558597
					0.3			1.2206695421
					0.4			1.2498660326
						0.8		1.2136554708
						1.0		1.2350042186
						1.2		1.2543002697
							0.2	1.1630229501
							0.3	1.1460058218
							0.4	1.1396650244

Fig. 11 depicts the influence of the Lewis number on the dimensionless nanoparticle volume concentration. It is noticed that the nanoparticle volume fraction experiences a strong reduction for larger Le values. The dimensionless Lewis number is defined as the ratio of thermal and mass diffusivity. By increasing the value of Le, the thermal boundary layer thickness is increased whereas the nanoparticle volume concentration boundary layer thickness is reduced.

As shows in table-2 the numerical values of Skin-friction coefficient for variations in values of the engineering parameters such as, M, S, λ, Pr, Nb, Nt, R and Le. From this table, it is observed that the Skin-friction coefficient is increasing with rising values of λ, Nb, Nt, R while it is decreasing with increasing values of M, S, Pr and Le.

For dissimilar values of Pr, R, Nb, and Nt. the numerical values of heat transfer rate coefficient are shown in Table-3. The rate of heat transfer coefficient increases as Nb and Nt values increase, while the reverse effect is observed in increasing values of Pr and *R*.

The effects of *Le*, *Nb* and *Nt* on rate of mass transfer coefficient or in terms Sherwood number coefficient are discussed in Table-4. From this table, it is observed that the rate of mass transfer coefficient is increasing with increasing values of *Nt* and decreasing with increasing values of Le and *Nb*.

Table-3.: Coefficients of heat transfer rates for different Pr, R, Nb, and Nt values

Pr	*R*	*Nb*	*Nt*	Nu_x
0.71	0.5	0.1	0.1	0.5480326154
1.0				0.4893326198
3.0				0.4690221069
7.0				0.4530098557
	0.8			0.5782231096
	1.0			0.6052230144
	1.2			0.6230220987
		0.2		0.5860012497
		0.3		0.6185540234
		0.4		0.6390221441
			0.2	0.5782203475
			0.3	0.5960114232
			0.4	0.6120040322

Table-4.: Different coefficients of heat transfer rates for different types of heat of *Sc* and *Sr*

Le	*Nb*	*Nt*	Sh_x
0.1	0.1	0.1	0.5632919824
0.3			0.5422923154

0.5			0.5132669563
0.8			0.5560399410
	0.3		0.5382201677
	0.5		0.5184487229
	0.8		0.4983326757
		0.3	0.5920031544
		0.5	0.6203995214
		0.8	0.6403329587

6. Conclusion

This study investigates the equilibrium of a viscous, incompressible, and electric fluid -state MHD flow as a result of thermal radiation non-Newtonian nanofluid over a non-linearly stretching sheet influenced through Brownian motion and Thermophoresis. The Runge-Kutta technique, which is a numerical technique, is used to elaborate the results. Some of the important findings in the study can be summarized in the following points.

1) The velocity profiles are increasing with an increasing in the values of Stretching sheet parameter.
2) The velocity profile decreases with rising values of Magnetic field parameter (M) and suction/injection parameters (S).
3) The temperature profile rise as the rising values Thermophoresis(Nt), Brownian Motion parameter(Nb) , Thermal radiation parameters(R).
4) Temperature profiles falling as the value of Prandtl number (Pr) increasing
5) The concentration profiles improve when the Thermophoresis parameter (Nt) is increased, while the Brownian motion parameter (Nb) and Lewis number parameter (Le) are reduced.
6) The present results are equalized with the previous work done by Magyari and Keller [18], Bidin and Nazar [19] and El-Aziz [21] are observed.

References

[1] Y. Lin, L. Zheng, X. Zhang, L. Ma, G. Chen, MHD pseudo-plastic nanofluid unsteady flow and heat transfer in a finite thin film over stretching surface with internal heat generation, *International Journal of Heat and Mass Transfer,* Vol. 84, pp. 903-911, 2015.

[2] C. Zhang, L. Zheng, X. Zhang, G. Chen, MHD flow and radiation heat transfer of nanofluids in porous media with variable surface heat flux and chemical reaction, *Applied Mathematical Modelling,* Vol. 39, No. 1, pp. 165-181, 2015.

[3] Y. Lin, L. Zheng, X. Zhang, Radiation effects on Marangoni convection flow and heat transfer in pseudo-plastic non-Newtonian nanofluids with variable thermal conductivity, *International Journal of Heat and Mass Transfer,* Vol. 77, pp. 708-716, 2014.

[4] F. Mabood, S. Ibrahim, M. Rashidi, M. Shadloo, G. Lorenzini, Non-uniform heat source/sink and Soret effects on MHD non-Darcian convective flow past a stretching sheet in a micropolar fluid with radiation, *International Journal of Heat and Mass Transfer,* Vol. 93, pp. 674-682, 2016.

[5] G. S. Seth, R. Sharma, B. Kumbhakar, A. J. Chamkha, Hydromagnetic flow of heat absorbing and radiating fluid over exponentially stretching sheet with partial slip and viscous and Joule dissipation, *Engineering Computations,* 2016.

[6] S. A. Devi, M. Prakash, Temperature dependent viscosity and thermal conductivity effects on hydromagnetic flow over a slendering stretching sheet, *Journal of the Nigerian Mathematical Society,* Vol. 34, No. 3, pp. 318-330, 2015.

[7] T. Hayat, G. Bashir, M. Waqas, A. Alsaedi, MHD 2D flow of Williamson nanofluid over a nonlinear variable thicked surface with melting heat transfer, *Journal of Molecular Liquids,* Vol. 223, pp. 836-844, 2016.

[8] T. Hayat, M. I. Khan, A. Alsaedi, M. I. Khan, Homogeneous-heterogeneous reactions and melting heat transfer effects in the MHD flow by a stretching surface with variable thickness, *Journal of Molecular Liquids*, Vol. 223, pp. 960-968, 2016.

[9] M. Farooq, M. I. Khan, M. Waqas, T. Hayat, A. Alsaedi, M. I. Khan, MHD stagnation point flow of viscoelastic nanofluid with non-linear radiation effects, *Journal of molecular liquids*, Vol. 221, pp. 1097-1103, 2016.

[10] M. I. Khan, T. Hayat, M. I. Khan, A. Alsaedi, A modified homogeneous-heterogeneous reactions for MHD stagnation flow with viscous dissipation and Joule heating, *International Journal of Heat and Mass Transfer*, Vol. 113, pp. 310-317, 2017.

[11] T. Hayat, M. I. Khan, M. Waqas, A. Alsaedi, Effectiveness of magnetic nanoparticles in radiative flow of Eyring-Powell fluid, *Journal of Molecular Liquids*, Vol. 231, pp. 126-133, 2017.

[12] T. Hayat, M. I. Khan, M. Waqas, T. Yasmeen, A. Alsaedi, Viscous dissipation effect in flow of magnetonanofluid with variable properties, *Journal of Molecular Liquids*, Vol. 222, pp. 47-54, 2016.

[13] T. Hayat, M. I. Khan, M. Farooq, A. Alsaedi, T. Yasmeen, Impact of Marangoni convection in the flow of carbon–water nanofluid with thermal radiation, *International Journal of Heat and Mass Transfer*, Vol. 106, pp. 810-815, 2017.

[14] T. Hayat, M. Tamoor, M. I. Khan, A. Alsaedi, Numerical simulation for nonlinear radiative flow by convective cylinder, *Results in physics*, Vol. 6, pp. 1031-1035, 2016.

[15] M. Tamoor, M. Waqas, M. I. Khan, A. Alsaedi, T. Hayat, Magnetohydrodynamic flow of Casson fluid over a stretching cylinder, *Results in physics*, Vol. 7, pp. 498-502, 2017.

[16] N. BABU, G. MURALI, S. BHATI, Casson fluid performance on natural convective dissipative couette flow past an infinite vertically inclined plate filled in porous medium with heat transfer, mhd and hall current effects, *International Journal of Pharmaceutical Research*, Vol. 10, No. 4, 2018.

[17] G. Murali, A. Paul, N. Babu, Heat and mass transfer effects on an unsteady hydromagnetic free convective flow over an infinite vertical plate embedded in a porous medium with heat absorption, *Int. J. Open Problems Compt. Math*, Vol. 8, No. 1, 2015.

[18] D. Gadipally, M. Gundagani, N. N. Babu, EFFECTS OF THERMAL RADIATION AND CHEMICAL REACTION ON UNSTEADY HYDROMAGNETIC MIXED CONVECTION FLOW PAST AN INFINITE VERTICAL PLATE, *Journal of Science and Arts*, Vol. 18, No. 3, pp. 763-776, 2018.

[19] M. Mohammadi, A. Farajpour, A. Moradi, M. Hosseini, Vibration analysis of the rotating multilayer piezoelectric Timoshenko nanobeam, *Engineering Analysis with Boundary Elements*, Vol. 145, pp. 117-131, 2022.

[20] M. Mohammadi, A. Rastgoo, Primary and secondary resonance analysis of FG/lipid nanoplate with considering porosity distribution based on a nonlinear elastic medium, *Mechanics of Advanced Materials and Structures*, Vol. 27, No. 20, pp. 1709-1730, 2020.

[21] M. Mohammadi, M. Hosseini, M. Shishesaz, A. Hadi, A. Rastgoo, Primary and secondary resonance analysis of porous functionally graded nanobeam resting on a nonlinear foundation subjected to mechanical and electrical loads, *European Journal of Mechanics-A/Solids*, Vol. 77, pp. 103793, 2019.

[22] M. Mohammadi, A. Rastgoo, Nonlinear vibration analysis of the viscoelastic composite nanoplate with three directionally imperfect porous FG core, *Structural Engineering and Mechanics, An Int'l Journal*, Vol. 69, No. 2, pp. 131-143, 2019.

[23] A. Farajpour, A. Rastgoo, M. Mohammadi, Vibration, buckling and smart control of microtubules using piezoelectric nanoshells under electric voltage in thermal environment, *Physica B: Condensed Matter*, Vol. 509, pp. 100-114, 2017.

[24] A. Farajpour, M. H. Yazdi, A. Rastgoo, M. Loghmani, M. Mohammadi, Nonlocal nonlinear plate model for large amplitude vibration of magneto-electro-elastic nanoplates, *Composite Structures*, Vol. 140, pp. 323-336, 2016.

[25] A. Farajpour, M. H. Yazdi, A. Rastgoo, M. Mohammadi, A higher-order nonlocal strain gradient plate model for buckling of orthotropic nanoplates in thermal environment, *Acta Mechanica*, Vol. 227, pp. 1849-1867, 2016.

[26] M. Mohammadi, M. Safarabadi, A. Rastgoo, A. Farajpour, Hygro-mechanical vibration analysis of a rotating viscoelastic nanobeam embedded in a visco-Pasternak elastic medium and in a nonlinear thermal environment, *Acta Mechanica*, Vol. 227, pp. 2207-2232, 2016.

[27] M. R. Farajpour, A. Rastgoo, A. Farajpour, M. Mohammadi, Vibration of piezoelectric nanofilm-based electromechanical sensors via higher-order non-local strain gradient theory, *Micro & Nano Letters,* Vol. 11, No. 6, pp. 302-307, 2016.

[28] M. Baghani, M. Mohammadi, A. Farajpour, Dynamic and stability analysis of the rotating nanobeam in a nonuniform magnetic field considering the surface energy, *International Journal of Applied Mechanics,* Vol. 8, No. 04, pp. 1650048, 2016.

[29] M. Goodarzi, M. Mohammadi, M. Khooran, F. Saadi, Thermo-mechanical vibration analysis of FG circular and annular nanoplate based on the visco-pasternak foundation, *Journal of Solid Mechanics,* Vol. 8, No. 4, pp. 788-805, 2016.

[30] H. Asemi, S. Asemi, A. Farajpour, M. Mohammadi, Nanoscale mass detection based on vibrating piezoelectric ultrathin films under thermo-electro-mechanical loads, *Physica E: Low-dimensional Systems and Nanostructures,* Vol. 68, pp. 112-122, 2015.

[31] M. Safarabadi, M. Mohammadi, A. Farajpour, M. Goodarzi, Effect of surface energy on the vibration analysis of rotating nanobeam, 2015.

[32] M. Goodarzi, M. Mohammadi, A. Gharib, Techno-Economic Analysis of Solar Energy for Cathodic Protection of Oil and Gas Buried Pipelines in Southwestern of Iran, in *Proceeding of,* https://publications.waset.org/abstracts/33008/techno-economic-analysis-of …, pp.

[33] M. Mohammadi, A. A. Nekounam, M. Amiri, The vibration analysis of the composite natural gas pipelines in the nonlinear thermal and humidity environment, in *Proceeding of,* https://civilica.com/doc/540946/, pp.

[34] M. Goodarzi, M. Mohammadi, M. Rezaee, Technical Feasibility Analysis of PV Water Pumping System in Khuzestan Province-Iran, in *Proceeding of,* https://publications.waset.org/abstracts/18930/technical-feasibility …, pp.

[35] M. Mohammadi, A. Farajpour, A. Moradi, M. Ghayour, Shear buckling of orthotropic rectangular graphene sheet embedded in an elastic medium in thermal environment, *Composites Part B: Engineering,* Vol. 56, pp. 629-637, 2014.

[36] M. Mohammadi, A. Moradi, M. Ghayour, A. Farajpour, Exact solution for thermo-mechanical vibration of orthotropic mono-layer graphene sheet embedded in an elastic medium, *Latin American Journal of Solids and Structures,* Vol. 11, pp. 437-458, 2014.

[37] M. Mohammadi, A. Farajpour, M. Goodarzi, F. Dinari, Thermo-mechanical vibration analysis of annular and circular graphene sheet embedded in an elastic medium, *Latin American Journal of Solids and Structures,* Vol. 11, pp. 659-682, 2014.

[38] M. Mohammadi, A. Farajpour, M. Goodarzi, Numerical study of the effect of shear in-plane load on the vibration analysis of graphene sheet embedded in an elastic medium, *Computational Materials Science,* Vol. 82, pp. 510-520, 2014.

[39] A. Farajpour, A. Rastgoo, M. Mohammadi, Surface effects on the mechanical characteristics of microtubule networks in living cells, *Mechanics Research Communications,* Vol. 57, pp. 18-26, 2014.

[40] S. R. Asemi, M. Mohammadi, A. Farajpour, A study on the nonlinear stability of orthotropic single-layered graphene sheet based on nonlocal elasticity theory, *Latin American Journal of Solids and Structures*, Vol. 11, pp. 1541-1546, 2014.

[41] M. Goodarzi, M. Mohammadi, A. Farajpour, M. Khooran, Investigation of the effect of pre-stressed on vibration frequency of rectangular nanoplate based on a visco-Pasternak foundation, 2014.

[42] S. Asemi, A. Farajpour, H. Asemi, M. Mohammadi, Influence of initial stress on the vibration of double-piezoelectric-nanoplate systems with various boundary conditions using DQM, *Physica E: Low-dimensional Systems and Nanostructures,* Vol. 63, pp. 169-179, 2014.

[43] S. Asemi, A. Farajpour, M. Mohammadi, Nonlinear vibration analysis of piezoelectric nanoelectromechanical resonators based on nonlocal elasticity theory, *Composite Structures,* Vol. 116, pp. 703-712, 2014.

[44] M. Mohammadi, M. Ghayour, A. Farajpour, Free transverse vibration analysis of circular and annular graphene sheets with various boundary conditions using the nonlocal continuum plate model, *Composites Part B: Engineering,* Vol. 45, No. 1, pp. 32-42, 2013.

[45] M. Mohammadi, M. Goodarzi, M. Ghayour, A. Farajpour, Influence of in-plane pre-load on the vibration frequency of circular graphene sheet via nonlocal continuum theory, *Composites Part B: Engineering,* Vol. 51, pp. 121-129, 2013.

[46] M. Mohammadi, A. Farajpour, M. Goodarzi, R. Heydarshenas, Levy type solution for nonlocal thermo-mechanical vibration of orthotropic mono-layer graphene sheet embedded in an elastic medium, *Journal of Solid Mechanics*, Vol. 5, No. 2, pp. 116-132, 2013.

[47] M. Mohammadi, A. Farajpour, M. Goodarzi, H. Mohammadi, Temperature Effect on Vibration Analysis of Annular Graphene Sheet Embedded on Visco-Pasternak Foundati, *Journal of Solid Mechanics,* Vol. 5, No. 3, pp. 305-323, 2013.

[48] S. Ghannadpour, B. Mohammadi, J. Fazilati, Bending, buckling and vibration problems of nonlocal Euler beams using Ritz method, *Composite Structures,* Vol. 96, pp. 584-589, 2013.

[49] M. Danesh, A. Farajpour, M. Mohammadi, Axial vibration analysis of a tapered nanorod based on nonlocal elasticity theory and differential quadrature method, *Mechanics Research Communications,* Vol. 39, No. 1, pp. 23-27, 2012.

[50] A. Farajpour, A. Shahidi, M. Mohammadi, M. Mahzoon, Buckling of orthotropic micro/nanoscale plates under linearly varying in-plane load via nonlocal continuum mechanics, *Composite Structures*, Vol. 94, No. 5, pp. 1605-1615, 2012.

[51] M. Mohammadi, M. Goodarzi, M. Ghayour, S. Alivand, Small scale effect on the vibration of orthotropic plates embedded in an elastic medium and under biaxial in-plane pre-load via nonlocal elasticity theory, 2012.

[52] A. Farajpour, M. Mohammadi, A. Shahidi, M. Mahzoon, Axisymmetric buckling of the circular graphene sheets with the nonlocal continuum plate model, *Physica E: Low-dimensional Systems and Nanostructures*, Vol. 43, No. 10, pp. 1820-1825, 2011.

[53] A. Farajpour, M. Danesh, M. Mohammadi, Buckling analysis of variable thickness nanoplates using nonlocal continuum mechanics, *Physica E: Low-dimensional Systems and Nanostructures,* Vol. 44, No. 3, pp. 719-727, 2011.

[54] H. Moosavi, M. Mohammadi, A. Farajpour, S. Shahidi, Vibration analysis of nanorings using nonlocal continuum mechanics and shear deformable ring theory, *Physica E: Low-dimensional Systems and Nanostructures*, Vol. 44, No. 1, pp. 135-140, 2011.

[55] M. Mohammadi, M. Ghayour, A. Farajpour, Analysis of free vibration sector plate based on elastic medium by using new version differential quadrature method, *Journal of solid mechanics in engineering*, Vol. 3, No. 2, pp. 47-56, 2011.

[56] A. Farajpour, M. Mohammadi, M. Ghayour, Shear buckling of rectangular nanoplates embedded in elastic medium based on nonlocal elasticity theory, in *Proceeding of,* www.civilica.com/Paper-ISME19-ISME19_390.html, pp. 390.

[57] M. Mohammadi, A. Farajpour, A. R. Shahidi, Higher order shear deformation theory for the buckling of orthotropic rectangular nanoplates using nonlocal elasticity, in *Proceeding of,* www.civilica.com/Paper-ISME19-ISME19_391.html, pp. 391.

[58] M. Mohammadi, A. Farajpour, A. R. Shahidi, Effects of boundary conditions on the buckling of single-layered graphene sheets based on nonlocal elasticity, in *Proceeding of,* www.civilica.com/Paper-ISME19-ISME19_382.html, pp. 382.

[59] M. Mohammadi, M. Ghayour, A. Farajpour, Using of new version integral differential method to analysis of free vibration orthotropic sector plate based on elastic medium, in *Proceeding of*, www.civilica.com/Paper-ISME19-ISME19_497.html, pp. 497.

[60] M. Mohammadi, A. Farajpour, A. Rastgoo, Coriolis effects on the thermo-mechanical vibration analysis of the rotating multilayer piezoelectric nanobeam, *Acta Mechanica,* Vol. 234, No. 2, pp. 751-774, 2023/02/01, 2023.

[61] E. Magyari, B. Keller, Heat and mass transfer in the boundary layers on an exponentially stretching continuous surface, *Journal of Physics D: Applied Physics,* Vol. 32, No. 5, pp. 577, 1999.

[62] B. Bidin, R. Nazar, Numerical solution of the boundary layer flow over an exponentially stretching sheet with thermal radiation, *European journal of scientific research,* Vol. 33, No. 4, pp. 710-717, 2009.

[63] M. Abd El-Aziz, Viscous dissipation effect on mixed convection flow of a micropolar fluid over an exponentially stretching sheet, *Canadian Journal of Physics,* Vol. 87, No. 4, pp. 359-368, 2009.